NASA CR-134478

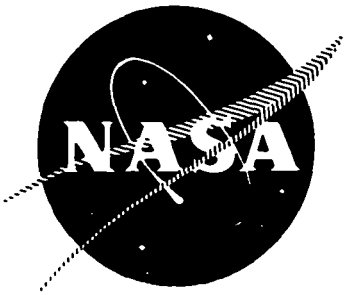

DROPLET BREAKUP IN ACCELERATING GAS FLOWS
PART I: PRIMARY ATOMIZATION

by
L. J. Zajac

ROCKETDYNE
A DIVISION OF ROCKWELL INTERNATIONAL
6633 CANOGA AVENUE, CANOGA PARK, CALIFORNIA

prepared for
NATIONAL AERONAUTICS AND SPACE ADMINISTRATION

NASA-Lewis Research Center
NAS3-14371

NOTICE

This report was prepared as an account of Government-sponsored work. Neither the United States, nor the National Aeronautics and Space Administration (NASA), nor any person acting on behalf of NASA:

A. Makes any warranty of representation, expressed or implied, with respect to the accuracy, completeness, or usefullness of the information contained in this report, or that the use of any information, apparatus, method, or process disclosed in this report may not infringe privately-owned rights; or

B. Assumes any liabilities with respect to the use of, or for damages resulting from the use of, any information, apparatus, method or process disclosed in this report.

As used above, "person acting on behalf of NASA" includes any employee or contractor of NASA, or employee of such contractor, to the extent that such employee or contractor of NASA or employee of such contractor prepares, disseminates, or provides access to any information pursuant to his employment or contract with NASA, or his employment with such contractor.

Requests for copies of this report should be referred to

National Aeronautics and Space Administration
Scientific and Technical Information Facility
P.O. Box 33
College Park, Md. 20740

1 Report No	2 Government Accession No	3 Recipient's Catalog No
NASA CR-134478		

4 Title and Subtitle	5 Report Date
DROPLET BREAKUP IN ACCELERATING GAS FLOWS PART I: PRIMARY ATOMIZATION	October 1973
	6 Performing Organization Code

7 Author(s)	8 Performing Organization Report No
L. J. Zajac	R-9337-1
	10 Work Unit No

9 Performing Organization Name and Address	11 Contract or Grant No
Rocketdyne Division, Rockwell International Canoga Park, California 91304	NAS3-14371
	13 Type of Report and Period Covered

12 Sponsoring Agency Name and Address	13 Type of Report and Period Covered
National Aeronautics and Space Administration Washington, D.C., 20546	Contractor Report
	14 Sponsoring Agency Code

15 Supplementary Notes

Technical Manager, R. J. Priem, NASA-Lewis Research Center, Cleveland, Ohio

16 Abstract

An experimental study of the effects of an accelerating gas flow on the atomization chracteristics of liquid sprays was conducted. The sprays were produced by impinging two liquid jets. The liquid was molten wax (Shell 270), while the gas was nitrogen. The use of molten wax allowed for a quantitative measure of the resulting dropsize distribution. The study was conducted in two parts. In one part, the effects of the gas on a cloud of drops was examined. The results of that study are presented in a companion volume, entitled "Droplet Breakup in Accelerating Gas Flows, Part II: Secondary Atomization" (R-9337-2). In the part of the study reported herein, the effects of the accelerating gas flow on the formation of the spray were examined. The results of this study indicate that the parameters that most affect the resulting dropsize are the injector parameters of orifice diameter and injection velocity, the maximum gas velocity, and the distance from the injector face at which the maximum gas velocity is attained. Empirical correlations for both the mass median dropsize and the dropsize distribution are presented. These correlations can be readily incorporated into existing computer codes for the purpose of calculating rocket engine combustion performance.

17 Key Words (Suggested by Author(s))	18 Distribution Statement
Droplet Breakup Primary Atomization Secondary Atomization Liquid Sprays Cold Flow Simulation Accelerating Gas Flows	

19 Security Classif (of this report)	20 Security Classif (of this page)	21 No of Pages	22 Price*
Unclassified	Unclassified	48	

* For sale by the National Technical Information Service, Springfield, Virginia 22151

Page Intentionally Left Blank

FOREWORD

The work described herein was conducted by Rocketdyne, a Division of Rockwell International, in accordance with the terms of Contract NAS3-14371 for the National Aeronautics and Space Administration, Lewis Research Center, Cleveland, Ohio. Dr. R. J. Priem of the Lewis Research Center served as the NASA Technical Manager. The Rocketdyne Program Manager was Mr. L. P. Combs. Technical guidance of the program was provided by Dr. D. T. Campbell. This report is presented in two volumes:

- NASA CR-134478--Part I: Primary Atomization (Rocketdyne internal report R-9337-1)

  NASA CR-134479--Part II: Secondary Atomization (Rocketdyne internal report R-9337-2)

Page Intentionally Left Blank

CONTENTS

Page Intentionally Left Blank

ILLUSTRATIONS

TABLES

Page Intentionally Left Blank

NOMENCLATURE

d	=	orifice diameter
D	=	droplet diamter
$\overline{D}$	=	mass median dropsize
$\overline{D}_c$	=	mass median dropsize when $V_{g_M} = V_L$
$\overline{D}_o$	=	mass median dropsize when $V_g = 0$
D_1	=	mass median dropsize produced by primary atomization process
L	=	gas acceleration ramp length
L_P	=	distance from injector to diffuser or gas acceleration ramp
T_g	=	gas temperature
T_L	=	liquid temperature
V_g	=	gas velocity
V_{g_o}	=	initial gas velocity
V_{g_M}	=	maximum gas velocity
V_L	=	liquid gas velocity
$\dot{w}$	=	mass flowrate
$\dot{w}_g$	=	gas flowrate
$\dot{w}_L$	=	liquid flowrate
α	=	flowrate ratio, $\dot{W}_L/\dot{W}_g$
ΔV	=	gas-to-liquid relative velocity, $V_{g_M} - V_L$
ρ_g	=	gas density
ρ_L	=	liquid density
τ	=	empirical parameter expressing influence of L on $\overline{D}$

1.0 SUMMARY

This report contains the results of an experimental study of the effects of an accelerating gas on the formation of a liquid spray. The spray was formed by the impingement of two liquid jets in an accelerating gaseous flowfield and the resulting mass median dropsizes were measured at several positions downstream of the impingement point. Molten wax was used as the liquid, and the gas was heated, ambient pressure nitrogen.

The experimental parameters that were varied included: the gas velocity, V_{g_M}, the distance from the impingement point to the maximum gas velocity location, L, and the injector variables of orifice diameter, d, and injection velocity, V_L. In terms of these parameters, the mass median dropsize of the spray, $\bar{D}_1$, can be expressed as *:

$$\bar{D}_1 = \tau \bar{D}_c \left[1 - 1.77\text{x}10^{-3} \bar{D}_c \left(\frac{V_{g_M} - V_L}{V_L}\right) \exp\left(-0.24 \frac{V_{g_M} - V_L}{V_L} \left|\frac{V_{g_M} - V_L}{V_L}\right|\right)\right]$$

over the range $-1 \leq \left(\frac{V_{g_M} - V_L}{V_L}\right) \leq 1.25$

and

$$\bar{D}_1 = \tau \left\{\bar{D}_c \left(1 - 1.52\text{x}10^{-3}\bar{D}_c\right) - 12 \ln\left(\frac{V_{g_M} - V_L}{V_L}\right)\right\}$$

for

$$\frac{V_{g_M} - V_L}{V_L} > 1.25$$

where

$$\bar{D}_c = 2.2\text{x}10^4 \, d^{0.375} \Big/ V_L^{0.75}$$

and

$$\tau = \left[1 + 7\text{x}10^5 \frac{\bar{D}_c V_L}{L} \sqrt{\frac{V_L}{V_{g_M}}}\right]^{0.41} ; \; L \geq 2 \text{ in.}$$

*$\bar{D}_1$ and $\bar{D}_c$ in microns, V_L and V_{g_M} in ft/sec, and d in inches.

In the above, V_{g_M} is the maximum gas velocity seen by the spray, i.e., the velocity at a distance L from the injector.

For large values of L, the parameter τ approaches unity and the empirical correlation for the dropsize, $\overline{D}_1$, reduces to the empirical function for the dropsize determined in the study of the secondary atomization process. This result implies that at sufficient distance from the injector, the influence of the gas on the spray formation can be neglected.

The above equations will yield erroneous results if used outside of the range of experimental data used in their development. For this reason, $\overline{D}_c$ should be limited to values between 140 and 360, V_{g_M} should be less than 1000 ft/sec, and L should not be less than 2 inches.

The dropsize distributions were found to become more nearly monodisperse as the mass median dropsize became smaller. A distribution function that was found to give a reasonably good fit to all of the data was the Rosin-Rammler normalized distribution function given by:

$$\frac{d\left[\dot{w}/\dot{w}_{TOT}\right]}{d\left[D/\overline{D}\right]} = \frac{2.46\ (D/\overline{D})^{1.46}}{(1.21)^{2.46}}\ \exp\left[-\frac{(D/\overline{D})^{2.46}}{1.61}\right]$$

where $\dot{w}/\dot{w}_{TOT}$ is the cumulative mass fraction of the spray having drop diameters smaller than D. In particular, this function gave an excellent fit in the large dropsize portion of the distribution curve.

2.0 INTRODUCTION

Droplet vaporization is often the rate-limiting process leading to combustion inefficiency in liquid rocket engines. The importance of liquid propellant spray dropsizes on combustion performance has been shown both analytically (Ref. 1 and 2) and experimentally (Ref. 3 through 7). However, the ability to analytically predict the combustion efficiency actually achieved under hot-firing conditions has been hampered because of insufficient experimental data describing the influence of combustion gas velocity on the spray produced by typical rocket engine injectors in finite length thrust chambers.

Extensive correlations between analytical performance predictions and hot-firing data (Ref.3 and 5) have identified the problem and indicated that the difference between experimental and calculated combustion efficiencies is, in fact, correlatable with combustion gas velocity. The velocity of the combustion gas can affect atomization by acting on either the sheet and ligaments during the formation of the spray (primary atomization) or the droplets themselves after the spray is formed (secondary atomization). The latter was the subject of an experimental cold-flow study conducted as a part of this same program. The results of that study are reported in Ref. 8. Contained herein are the results of another part of the program, e.g., the investigation of the effects of an accelerating gas on the primary atomization process.

Page Intentionally Left Blank

3.0 EXPERIMENTAL APPROACH

A detailed description of the test apparatus, data acquisition, and reduction techniques and data repeatability is presented in the report covering the secondary atomization (Ref. 8). However, to provide an understanding of the approach, a brief description will be presented here.

The apparatus that was used to perform the experiments is illustrated schematically in Fig. 1. The components of this apparatus are: (1) a single-element, like-doublet injector, through which the liquid is injected into the gas stream, (2) a constant area (10- by 10-inch) duct, (3) removable ramps which provide various gas acceleration rates, and (4) a diffuser which decelerates the two-phase flow and exhausts it into the atmosphere. Molten wax was used as the propellant simulant and gaseous nitrogen as the combustion gas simulant. To ensure that the molten wax did not solidify within the test section, the nitrogen was maintained at a temperature above the melting point of the wax (i.e., >140 F). The wax droplets were collected on an 18- by 50-foot water-flushed table, vacuum dried, and then subjected to a sieve analysis to determine the dropsize distribution and mass median dropsize. A data reproducibility of ±12 percent on the mass median dropsize was established for this experimental technique by repeat experiments under identical gas and liquid flow conditions.

Three ramp lengths, L, were utilized: 2, 4, and 8 inches. These ramps and the diffuser could be removed from the test section for constant gas velocity tests. Since the ramps had a fixed contraction ratio (5:1), the initial gas velocity, V_{g_o}, could not be varied independently of the maximum gas velocity, V_{g_M}.

The tests were conducted with three nominal flowrates (2, 4, and 8 lbm/sec) that provided gas velocity variations within the converging section from 50 to 250, 100 to 500, and 150 to 950 ft/sec, respectively.

Three like-doublet injectors were tested. During the tests, the injectors were positioned so that the impingement point coincided with the start of convergence. Their diameters, d, and the corresponding injection velocities, V_L, are listed in Table I. In addition, a characteristic dropsize of the injector, $\bar{D}_o$, is also given in the table. This dropsize was determined from the relation (Ref. 9):

$$\bar{D}_o = 15.9 \times 10^4 \, d^{0.57}/V_L \qquad (1)$$

and is the dropsize that would be obtained in the absence of a gas flow. In Eq. 1, $\bar{D}_o$ is in microns, d in inches, and V_L in ft/sec.

The injectors used in these experiments were designed to present a small cross section to the gas flow. As shown in Fig. 2, the injector orifices were contained in a long (9 inches), thin body to ensure that the liquid is injected into a relatively undisturbed gas stream. The particular injector

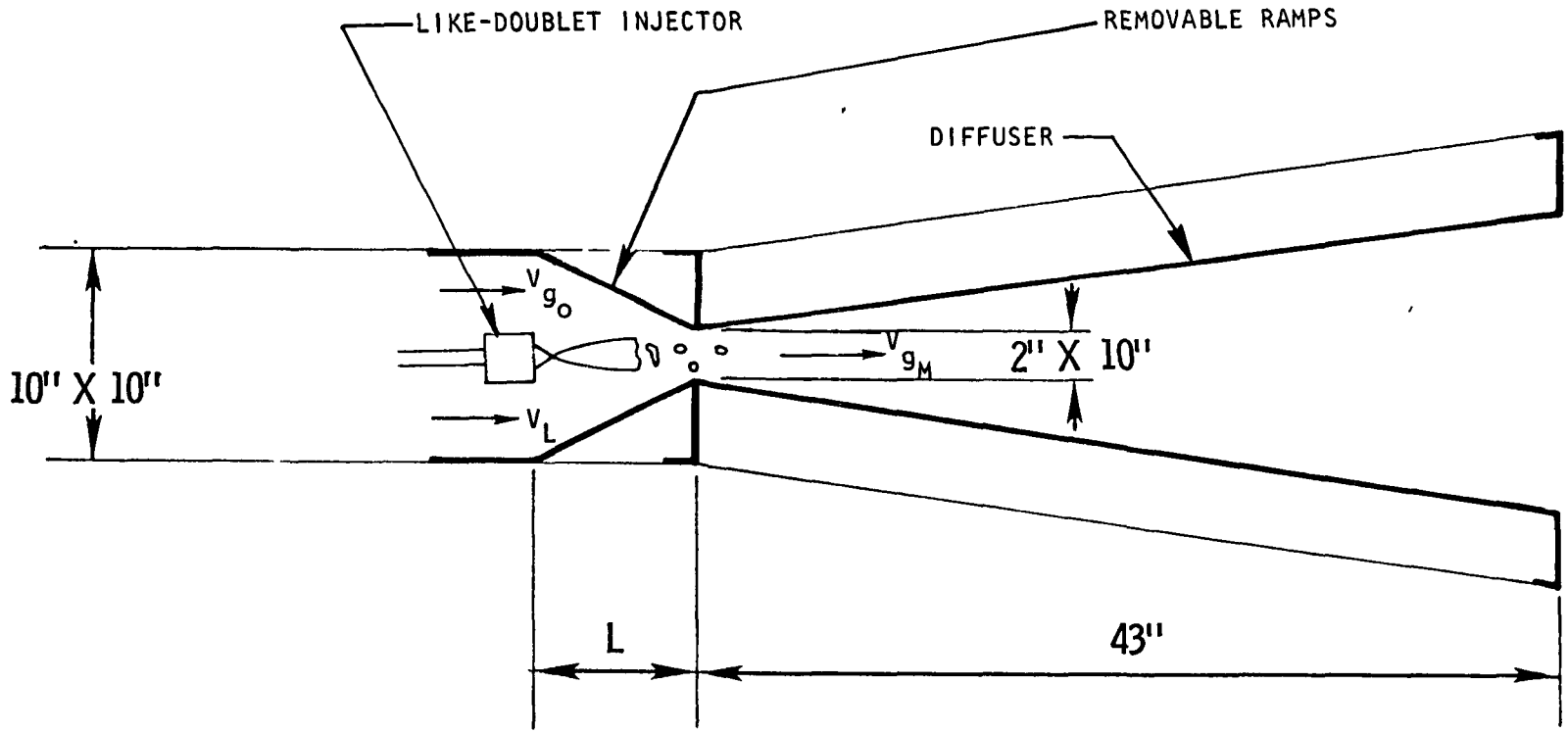

LIQUID: MOLTEN WAS (SHELL 270, T = 200 F)
GAS: NITROGEN(140 ≤ T ≤ 250 F)

Figure 1. Schematic Diagram of Test Section

TABLE I. LIKE-DOUBLET INJECTOR TESTS

Orifice Diameter (d), inch	Injection Velocity (V_L), ft/sec	Characteristic Dropsize ($\bar{D}_o$), microns
0.055	76	348
	160	191
0.094	142	292
	250	163
0.162	166	340

shown in Fig. 2 is the 0.094-inch-diameter element. The impingement angle for all injectors was 60 degrees, with a free-stream length/diameter ratio of about 5.

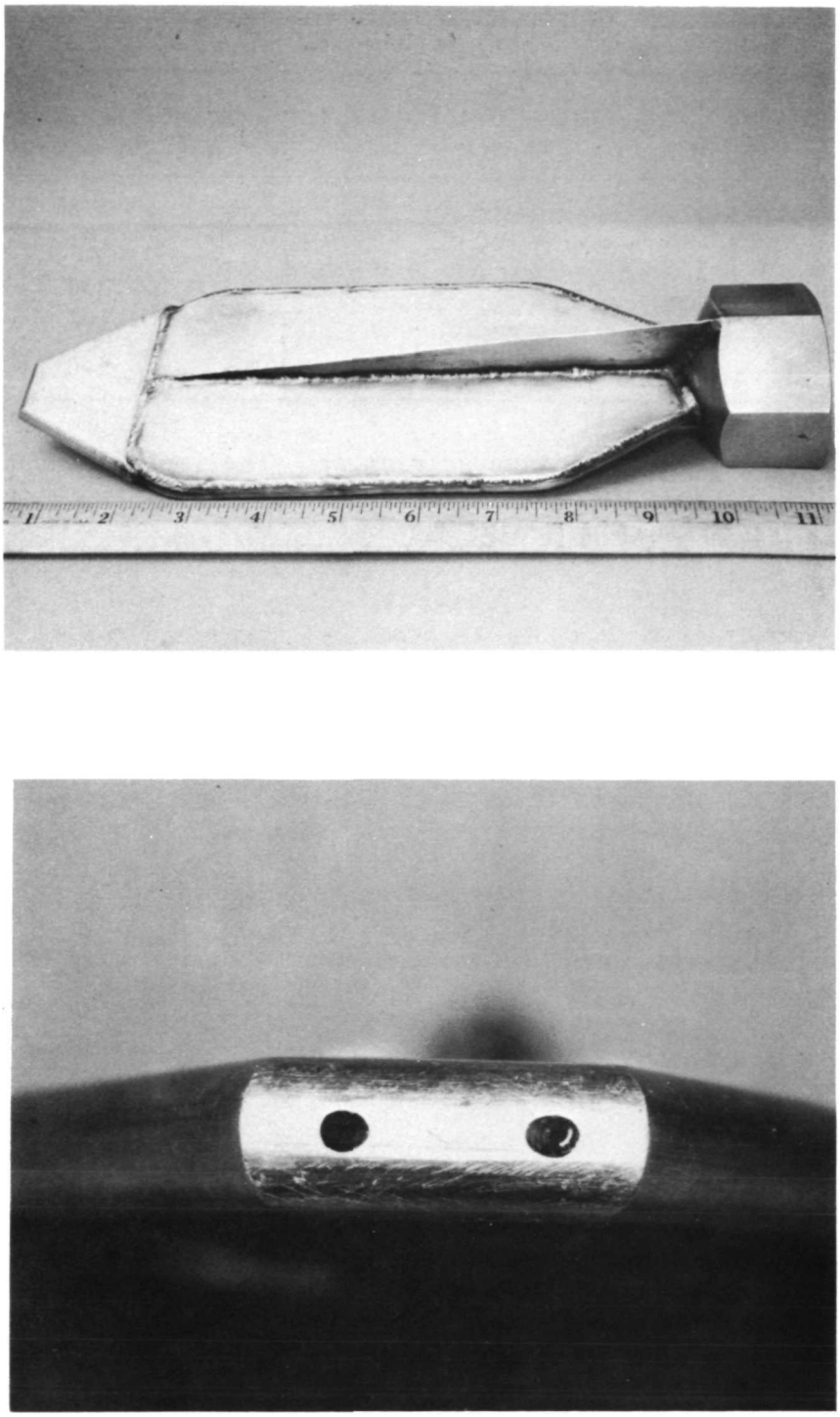

Figure 2. Typical Like-Doublet Injector Used in Atomization Study

4.0 EXPERIMENTAL RESULTS

The experimental parameters that were varied in the atomization experiments were the injector orifice diameter and injection velocity, the gas velocity profile, and the distance over which the spray was exposed to the accelerating gas flow. A total of 63 molten wax tests was conducted, 44 of which were with an accelerating gas flow. In the remaining 19 tests, the gas velocity was constant; the distance over which the spray was exposed to the constant gas velocity was 10 inches, a distance which was found to be sufficiently long to ensure the completion of the atomization process at that gas velocity (Ref. 8). The test conditions and the measured mass median dropsizes are listed in Table II (constant gas flow) and Table III (accelerating gas flow).

The effects of variations of the experimental parameters on both the mass median dropsize and the dropsize distribution were examined. The results for these two characteristic parameters of the spray are presented separately in the following paragraphs.

MASS MEDIAN DROPSIZE RESULTS

Influence of Gas Acceleration Distance

The results obtained by varying the distance over which the accelerating gas flow acted on the spray are shown in Fig. 3 through 5 for the 0.055-, 0.094-, and 0.162-inch-diameter elements, respectively. The maximum gas velocities, i.e., the gas velocity at the distance, L, from the injector face, are also indicated in the figures.

Most of the data show a decrease in the mass median dropsize when the ramp length was increased at a constant maximum gas velocity. The trend was observed with all three elements and changes up to 20 percent in the median dropsize were measured over distances of 2 to 8 inches. Although this change in the median dropsize is on the order of the range of data scatter expected ($\approx$12 percent) it is not believed to be a result of experimental error since an increase in the dropsize with distance was observed in only two cases. These occurred with the 0.055-inch-diameter orifice at a gas velocity of 500 ft/sec (Fig. 3a) and with the 0.094-inch-diameter orifice at a gas velocity of 150 ft/sec (Fig. 4b). In all other cases, the dropsize either remained constant or decreased as the length was increased.

Although dropsizes were not examined at gas acceleration distances greater than 8 inches, it is believed that no additional atomization would occur. As will be shown later, the median dropsizes obtained at this distance correspond very closely to those measured under similar gas and liquid conditions in the study of secondary atomization (Ref. 8) where it was found that acceleration distance had little effect on the median dropsize. Since it is almost certain that the spray is entirely formed at this distance from the injector (and the maximum gas velocity is no longer affecting the formation of the spray), the median dropsize should behave in a manner identical to that of the Ref. 8 study. Thus, the dropsize measured at 8 inches should represent essentially a limiting dropsize.

TABLE II. SUMMARY OF CONSTANT GAS VELOCITY TESTS

d, inch	V_L, ft/sec	$\dot{W}_L$, lb/sec	$\dot{W}_L/\dot{W}_g$	V_g, ft/sec	T_L, F	T_g, F	$\bar{D}_o$, microns	$\bar{D}_1$, microns
0.055	76	0.125	0.043	69	210	150	348	343
↓	76	↓	0.0286	98	205	163	↓	305
↓	76	↓	0.021	131	215	148	↓	262
↓	152	0.250	0.086	67	215	153	191	210
↓	152	0.250	0.086	70	210	173	191	208
↓	152	0.250	0.043	130	215	182	191	178
0.094	142	0.66	0.45	33	205	156	290	275
↓	↓	↓	0.226	67	200	170	↓	326
↓	↓	↓	0.151	97	215	150	↓	240
↓	↓	↓	0.113	129	215	183	↓	213
↓	↓	↓	0.090	154	210	190	↓	204
↓	250	1.06	0.090	35	205	170	163	285
↓	↓	↓	0.362	68	210	163	↓	223
↓	↓	↓	0.362	100	210	142	↓	204
↓	↓	↓	0.181	128	205	190	↓	230
↓	↓	↓	0.181	160	215	190	↓	184
0.162	166	2.26	0.774	70	205	145	340	350
0.162	166	2.26	0.516	95	210	163	340	335
0.162	166	2.26	0.387	123	210	142	340	280

Influence of Gas Velocity

The influence of the gas velocity on the mass median dropsize is illustrated in Fig. 6 and 7. These data were obtained with the 0.094-inch-diameter element at injection velocities of 142 and 250 ft/sec which, according to Eq. 1, corresponds to mass median dropsizes of 292 and 163 microns in still air (i.e., $V_g = 0$). The dropsize is shown as a function of the nondimensional velocity $(V_{g_M} - V_L)/V_L$ where V_{g_M} is the maximum velocity attained in the test section. However, since the liquid velocity, V_L, is constant for a given set of data, the variation of $\bar{D}_1$ is essentially due to the gas velocity. Also shown in the figures are the data obtained at constant gas velocities (solid symbols). The distance, L, for these tests was 10 inches, which was found to be a sufficient length for the completion of atomization. The distances for the accelerating gas flow experiments are differentiated by the various open symbols. The equation referred to in the figures will be explained below.

The data show, first of all, that the mean dropsize decreases rapidly with increasing gas velocity until the gas velocity attains a value of about twice the liquid velocity ($\Delta V/V_L = 1$). Further increases in the gas velocity produce only relatively small further decreases in the mean dropsize. The figures also show (noted previously in Fig. 3 through 5) that the dropsize is inversely

TABLE III. SUMMARY OF VARIABLE GAS VELOCITY TESTS

d, inch	V_L, ft/sec	$\dot{W}_L$, lb/sec	$\dot{W}_L/\dot{W}_g$	V_{g_o}, ft/sec	V_{g_M}, ft/sec	$V_{g_M} - V_L$, ft/sec	T_L, F	T_g, F	L, inch	$\bar{D}_o$, microns	$\bar{D}_1$, microns
0.094	142	0.66	0.66	30	152	10	205	310	2	292	255
				29	148	6	215	277	4		210
				30	148	6	225	280	8		200
				30	148	6	200	280	8		215
			0.33	52	250	108	220	155	2		218
				52	250	108	225	148	8		157
				52	250	108	215	160	8		156
				52	250	108	220	147	8		147
			0.16	93	485	343	220	157	2		165
			0.16	94	490	348	220	165	8		140
			0.08	155	1050	908	220	280	4		119
0.055	76	0.125	0.125	28	140	64	215	225	2	348	229
			0.125	28	140	64	222	218	8		216
			0.03	95	505	429	208	180	2		186
			0.03	95	505	429	210	180	4		155
			0.03	95	500	420	215	174	8		168
			0.015	151	1020	944	212	255	2		144
			0.015	145	970	890	220	215	8		135
0.162	166	2.26	2.26	30	150	-16	215	290	2	340	355
			2.26	53	155	-11	214	170	8		310
			1.13	52	255	89	220	330	8		205
			0.56	96	510	344	220	190	2		185
			0.56	96	510	344	205	185	4		175
			0.56	94	495	329	207	170	8		155
			0.28	153	1035	869	206	265	2		159
			0.28	154	1045	879	210	275	8		139
0.094	250	1.06	1.06	30	150	-100	220	280	2	163	252
				29	145	-105	215	263	4		265
				25	125	-125	237	135	8		260
				30	150	-100	205	285	8		220

TABLE III. (Concluded)

d, inch	V_L, ft/sec	$\dot{W}_L$, lb/sec	$\dot{W}_L/\dot{W}_g$	V_{g_o}, ft/sec	V_{g_M}, ft/sec	$V_{g_M} - V_L$ ft/sec	T_L, F	T_g, F	L, inch	$\overline{D}_o$, microns	$\overline{D}_1$, microns
0.094	250	1.06	0.53	51	240	-10	223	130	2	163	194
			0.53	52	250	0	210	150	8		157
			0.262	93	480	230	200	162	2		145
				93	480	230	225	165	2		160
				94	495	245	223	170	4		140
				96	510	260	220	190	8		130
			0.131	156	1065	815	205	290	2		127
			0.131	153	1035	785	225	265	8		102
0.055	160	0.250	0.250	28	140	-20	200	220	2	191	200
			0.250	27	135	-25	220	197	8		183
			0.0616	94	495	335	223	170	2		140
			0.0616	95	500	340	220	176	8		135
			0.031	147	985	825	220	228	2		124
			0.031	153	930	770	220	185	8		113

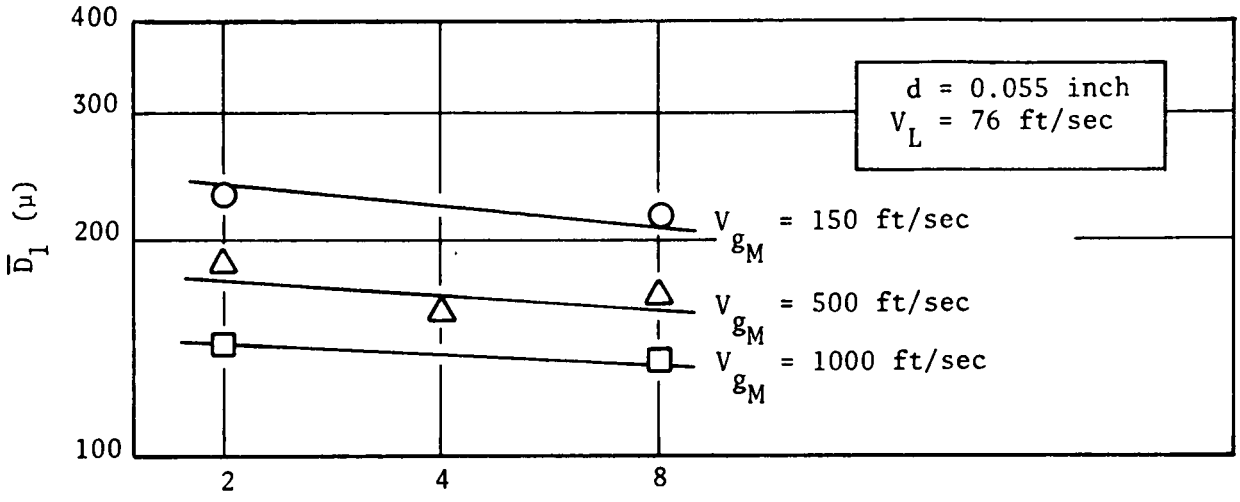

(a)

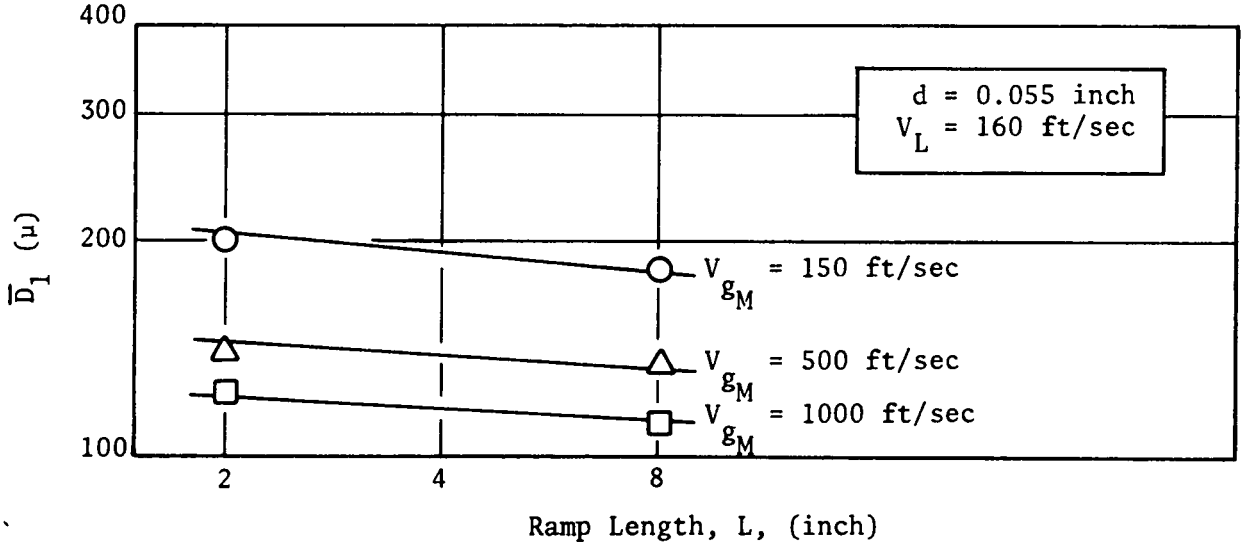

(b)

Figure 3. Influence of Ramp Length on the Mass Median Dropsize; d = 0.055 Inch

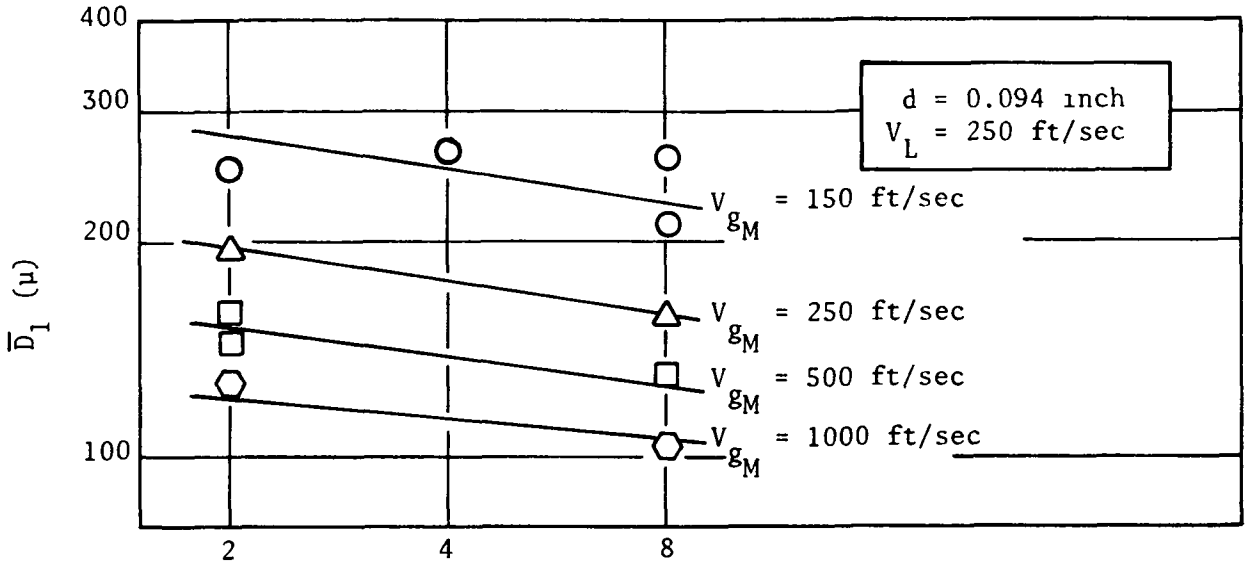

(a)

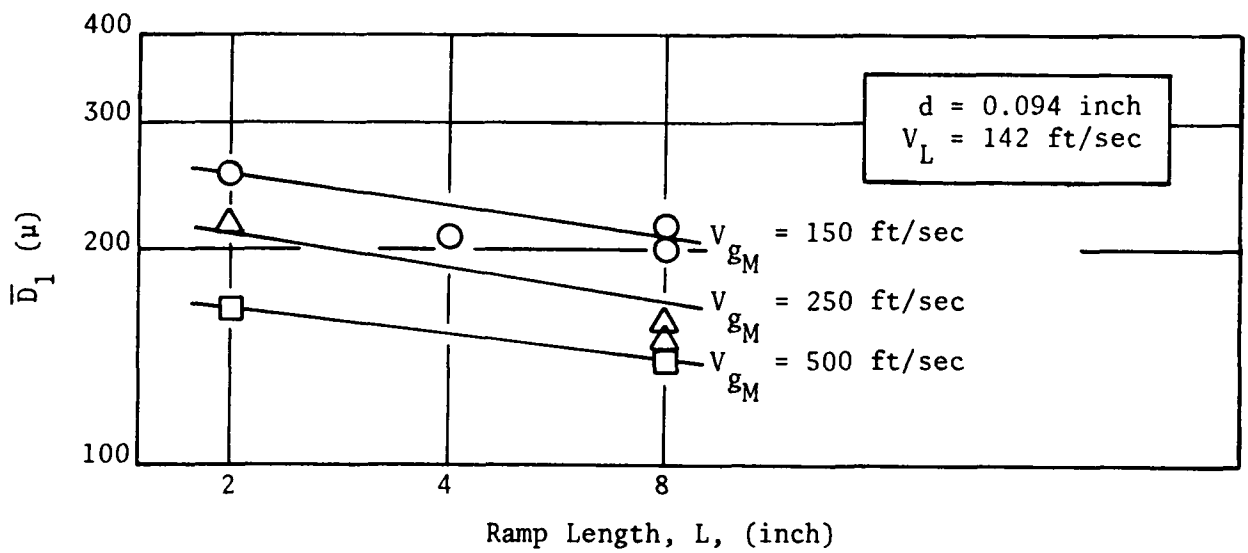

(b)

Figure 4. Influence of Ramp Length on the Mass Median Dropsize; d = 0.094 Inch

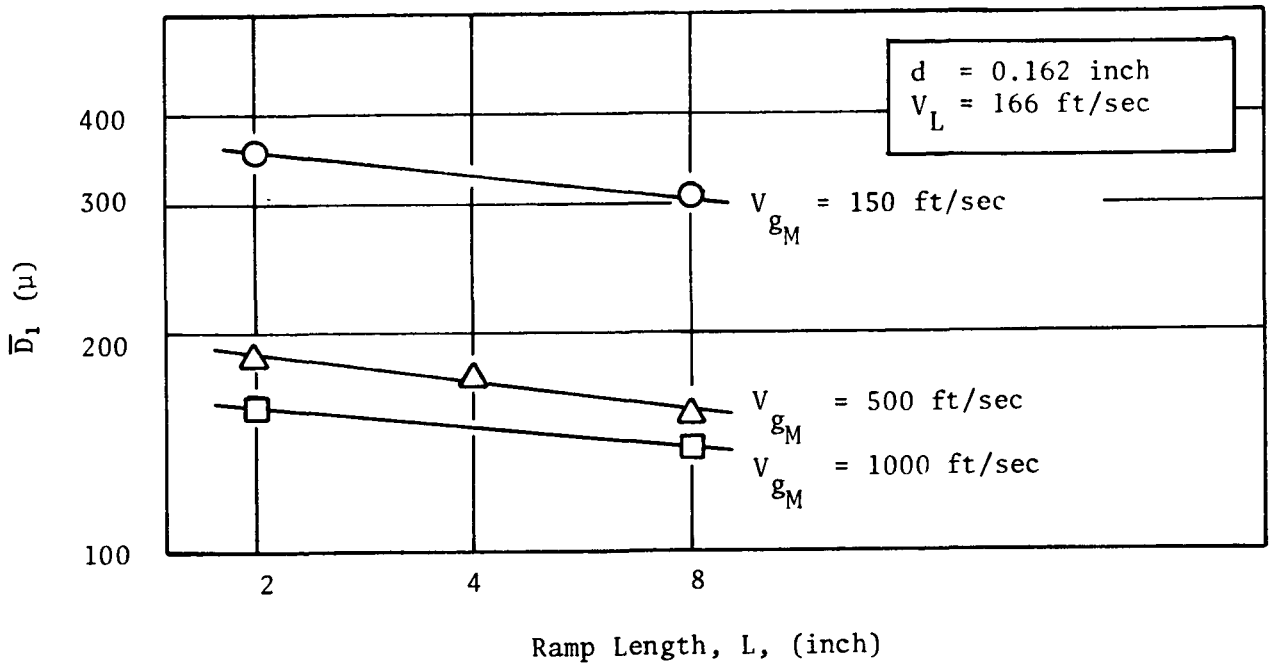

Figure 5. Influence of Ramp Length on the Mass Median Dropsize; d = 0.162 Inch

proportional to the distance (from the injector) where the maximum gas velocity is attained. (This is also the distance over which the liquid is exposed to the accelerating gas flowfield).

The dropsizes obtained at constant gas velocities (also shown in Fig. 6 and 7) were, in all cases, equal to or less than the dropsizes obtained when the gas was accelerated to the same maximum velocity over a finite length. A spray formed in a constant gas velocity thus appears to represent the lower value of the mean dropsize for a given V_{g_M}. Unfortunately, this comparison could not be made at higher gas velocities since facility flowrate limitations prevented the attainment of gas velocities in excess of about 200 ft/sec in the 10- by 10-inch constant area duct. Nevertheless, it is reasonable to expect that the "constant gas velocity dropsize" will still represent the lower limit at higher gas velocities.

An interesting aspect of the data is that a maximum dropsize did not occur when V_g was equal to V_L in the constant gas velocity cases. A maximum might be expected to occur at that condition because, at a zero relative velocity, no drag forces that would cause breakup are exerted on either the liquid sheet, ligaments, or droplets.* The dropsize did, however, exhibit a tendency to increase as the gas velocity was raised from zero. This is especially evident in Fig. 7 where it can be seen that, between a $\Delta V/V_L$ of from -1 to 0, all of the mean dropsizes obtained with a gas flow were larger than the dropsize obtained with no gas flow (closed triangle).

*It should be noted that the injectors were designed to minimize gas flow blockage and, hence, produce little disruption in the flowfield.

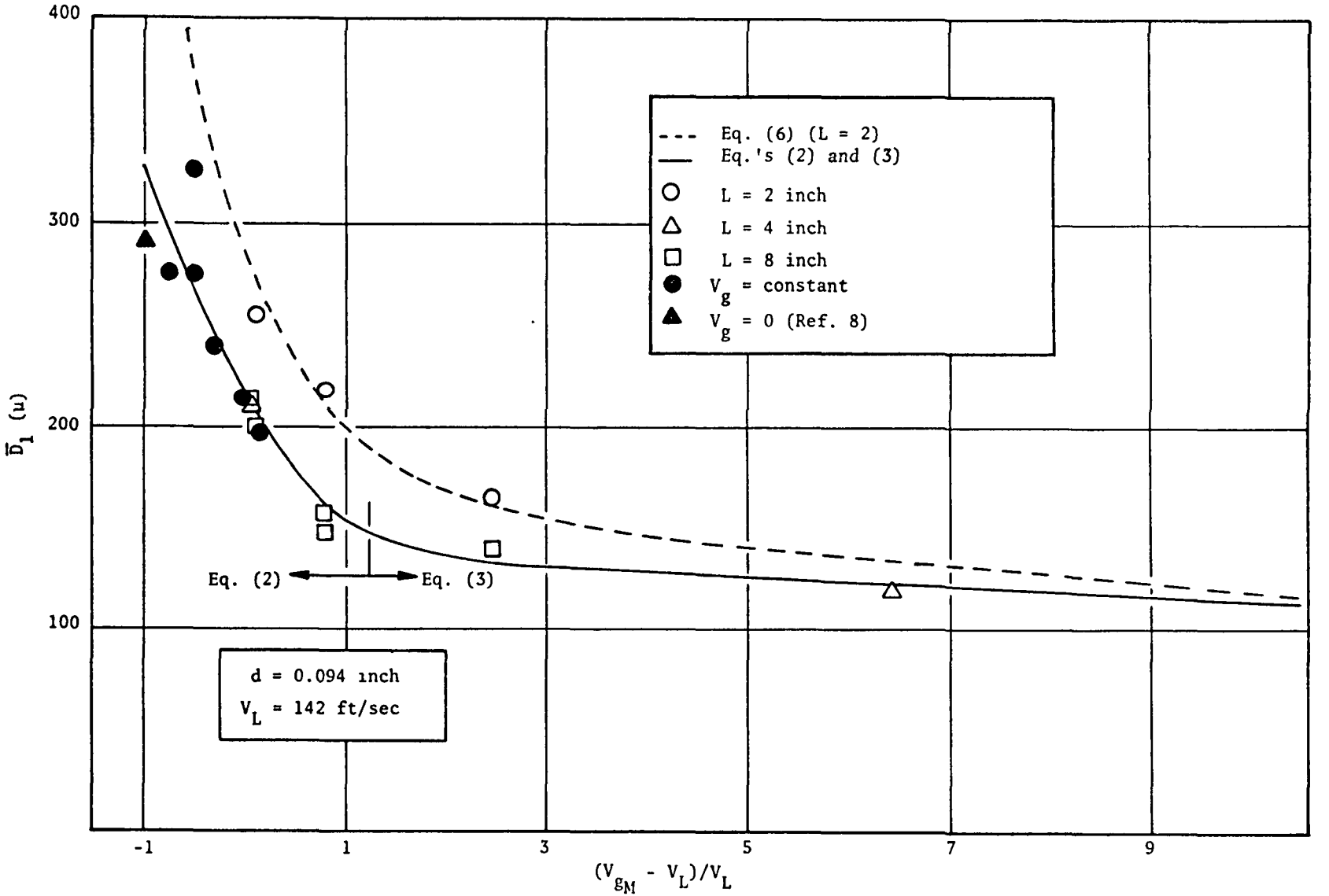

Figure 6. Influence of Gas Velocity on Mass Median Dropsize; $\bar{D}_o$ = 292 Microns

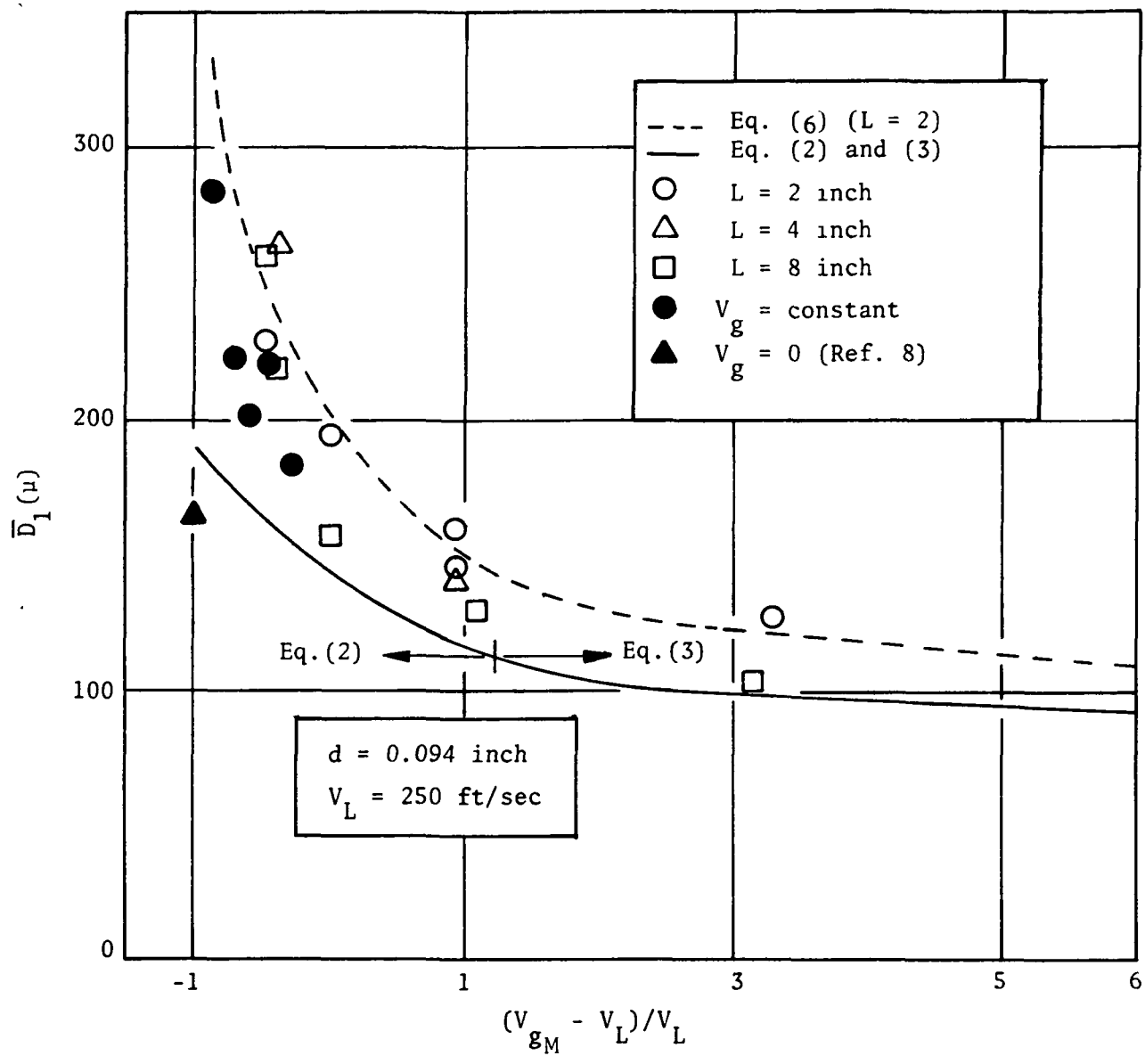

Figure 7. Influence of the Gas Velocity on the Mass Median Dropsize; $\overline{D}_o$ = 163 Microns

No definitive explanation can be given for this apparent anomoly. However, it is worth noting that the zero gas-to-liquid ΔV based on the mean injection and flow velocities does not mean that all ΔV's are zero everywhere in the flow-field. This results from the angular impingement of the jets which causes the spray to "fan out." Thus, at any gas velocity, including $V_g = V_L$, part of the spray sees a nonzero relative velocity and the maximum mean dropsize may occur at a minimum mass-averaged relative velocity. Since the spray mass and velocity vector distributions were not measured, this aspect of the data could not be examined in more detail.

It is of interest at this point to discuss briefly the results obtained in the study of the secondary atomization process that are presented in Ref. 8. In that study, the effects of the gas velocity and injector parameters (among other variables) on the atomization process were examined using a technique very similar to the one employed here. The basic difference was that the spray was allowed to form prior to being exposed to the accelerating gas by placing the injector a distance of 10 inches upstream of the gas acceleration zone. Thus, the dropsizes measured resulted from secondary droplet breakup and not because of a primary action of the gas on the breakup of liquid sheets and ligaments.

The empirical correlations developed for this "secondary" dropsize, $\bar{D}_2$, are given by *:

$$\bar{D}_2 = \bar{D}_c \left[1 - 1.77\text{x}10^{-3} \bar{D}_c \left(\frac{\Delta V}{V_L} \right) \exp \left(-0.24 \frac{\Delta V}{V_L} \left| \frac{\Delta V}{V_L} \right| \right) \right] \tag{2}$$

for the range $-1 \leq \frac{\Delta V}{V_L} \leq 1.25$

and

$$\bar{D}_2 = \bar{D}_c \left[1 - 1.52\text{x}10^{-3} \bar{D}_c \right] -12 \ln \left(\frac{\Delta V}{V_L} \right) \tag{3}$$

for $\frac{\Delta V}{V_L} > 1.25$

where $\frac{\Delta V}{V_L} = \frac{V_{g_M} - V_L}{V_L}$

and $\bar{D}_c = 2.2\text{x}10^4 \, d^{0.375} / V_L^{0.75}$ (4)

---

*$\bar{D}_2$ and $\bar{D}_1$ in microns; V_g amd V_L in ft/sec; d in inches

Equations 2 and 3 are represented, over their appropriate ranges of $\Delta V/V_L$, in Fig. 6 and 7 by solid lines. It can be seen that the data obtained in this study, at an exposure distance of 8 inches, agree quite well with the above correlations even though these data were obtained with the liquid being injected directly into the accelerating gas flow. The conclusion that must be reached, therefore, is that at this distance the median dropsize is dominated by the secondary atomization process. When the same maximum velocity is achieved within shorter distances, the median dropsizes become larger, as shown in Fig. 6 and 7 (and previously in Fig. 3 through 5). This increase must be attributed, at least partly, to the influence of the gas acceleration on the spray formation since, for the secondary atomization process, a much smaller effect of length was observed.

Since the data appear to be reaching a limiting dropsize, with a value given by either Eq. 2 or 3, an empirically determined multiplier to these equations was detérmined to account for the increase in dropsize with reduced (exposure) distance. This factor is given by:

$$\tau = \left[1 + 7\times10^{-5} \frac{\overline{D}_c V_L}{L} \sqrt{\frac{V_L}{V_{g_M}}}\right]^{0.41} \tag{5}$$

where $\overline{D}_c$ is given by Eq. 4. The dropsize at any distance greater than 2 inches from the injector, $\overline{D}_1$, is then given by:

$$\overline{D}_1 = \overline{D}_2 \ \tau \tag{6}$$

where $\overline{D}_2$ is determined from Eq. 2 and 3. As shown in Fig. 6 and 7, Eq. 6 with L = 2 inches (dashed lined) agrees well with the data obtained at a distance of 2 inches.

Similar results were obtained with the other element sizes. The data obtained with the 0.055-inch-diameter element (shown in Fig. 8) also compared well with the correlation provided by Eq. 6, as did the data obtained with the 0.162-inch-diameter element (shown in Fig. 9). In all cases, the dropsize varied inversely with the distance at which the maximum gas velocity was achieved. Also, the dropsize appears to be approaching a maximum at a gas velocity somewhere between 0 and V_L for these injectors as well.

Influence of Orifice Diameter and Injection Velocity

The effect on the mass median dropsize of variations in the orifice diameter is shown in Fig. 10. For these data, the liquid injection velocity was about 150 ft/sec and the dropsizes were determined after an exposure distance, L, of 8 inches. The data show that the median dropsize increases with orifice diameter, but also that this parameter becomes of lesser importance to the

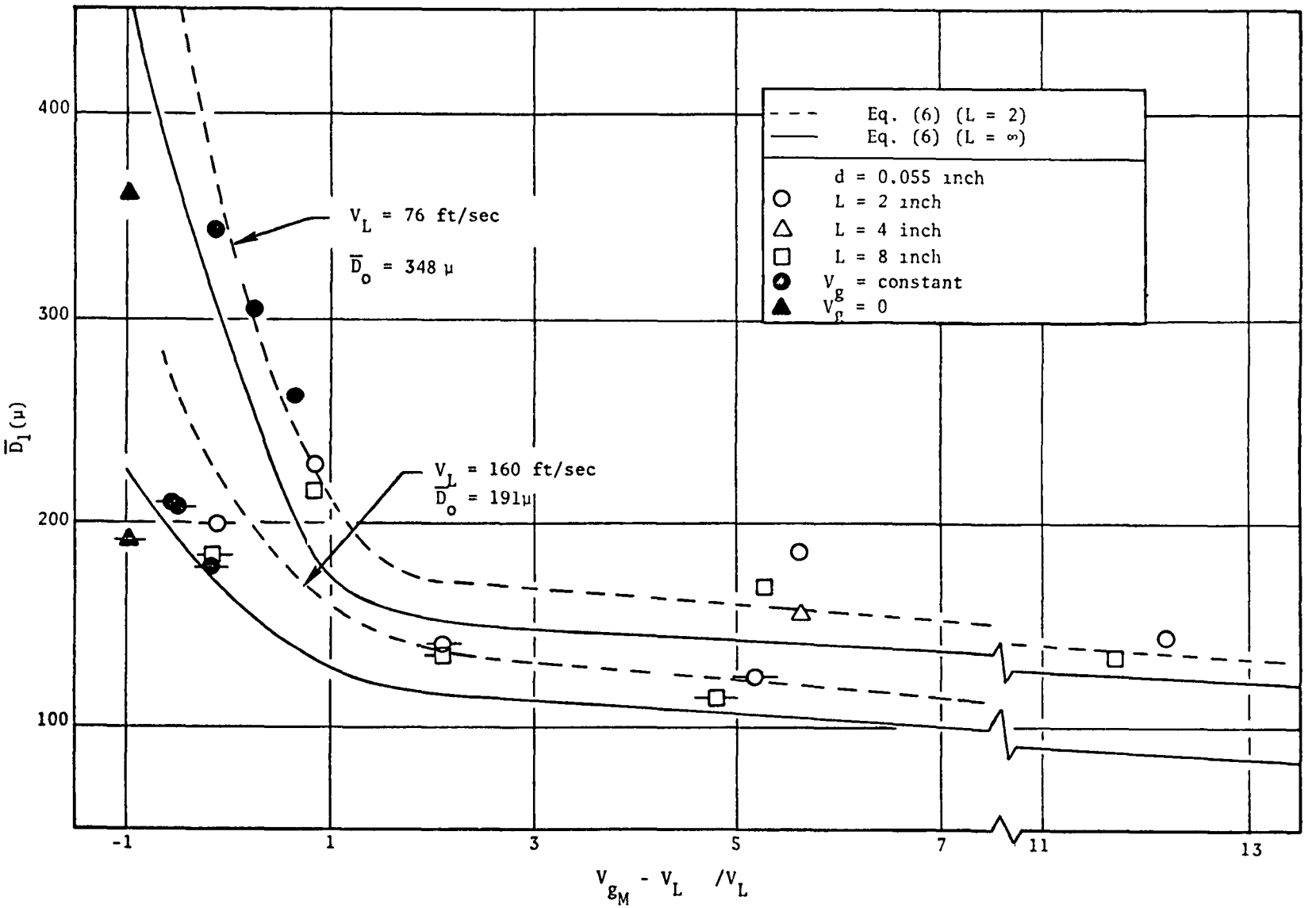

Figure 8. Influence of the Gas Velocity on the Mass Median Dropsize; $\overline{D}_o$ = 348 microns and 191 microns

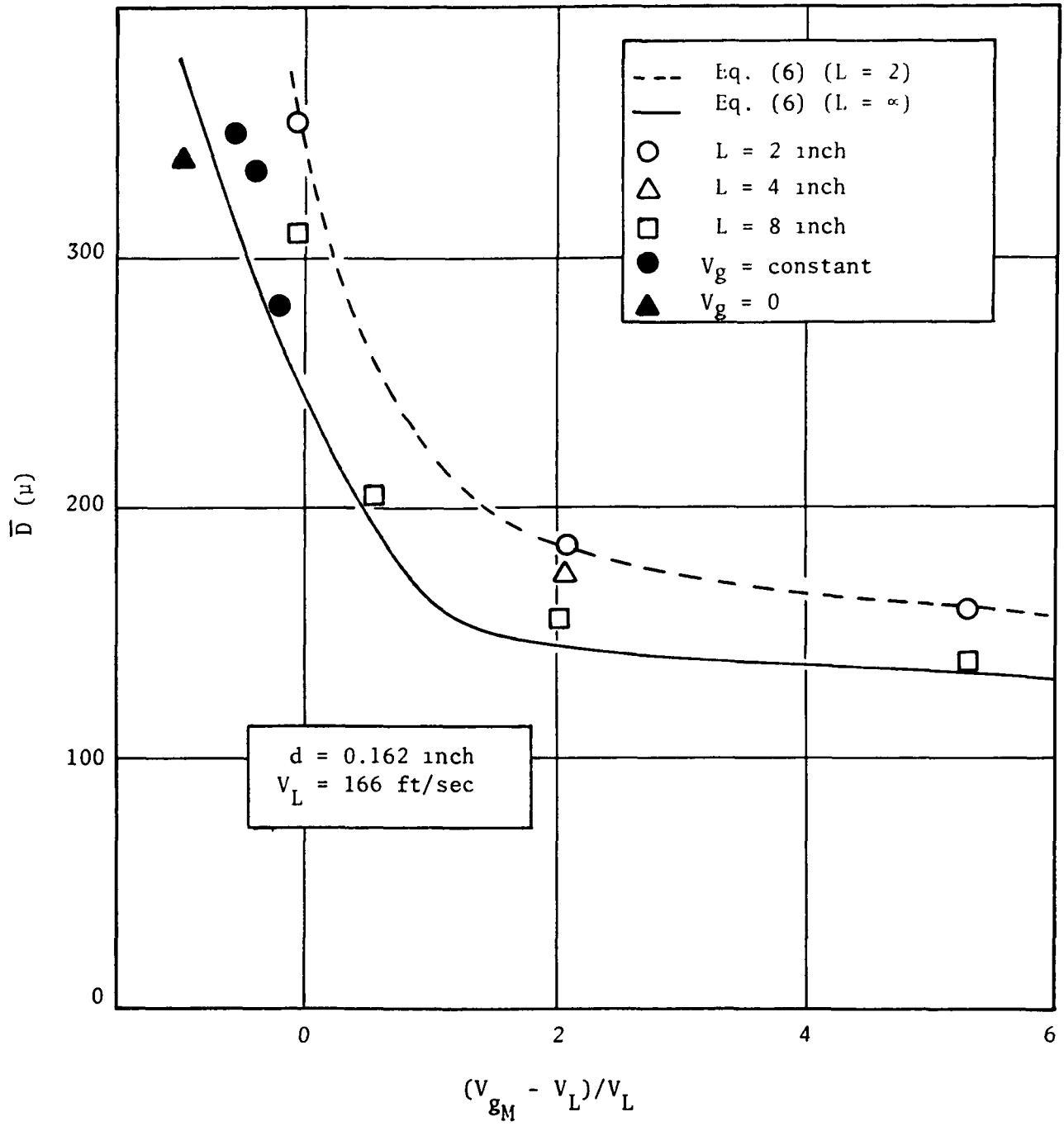

Figure 9. Influence of the Gas Velocity on the Mass Median Dropsize; $\bar{D}_o$ = 340 microns

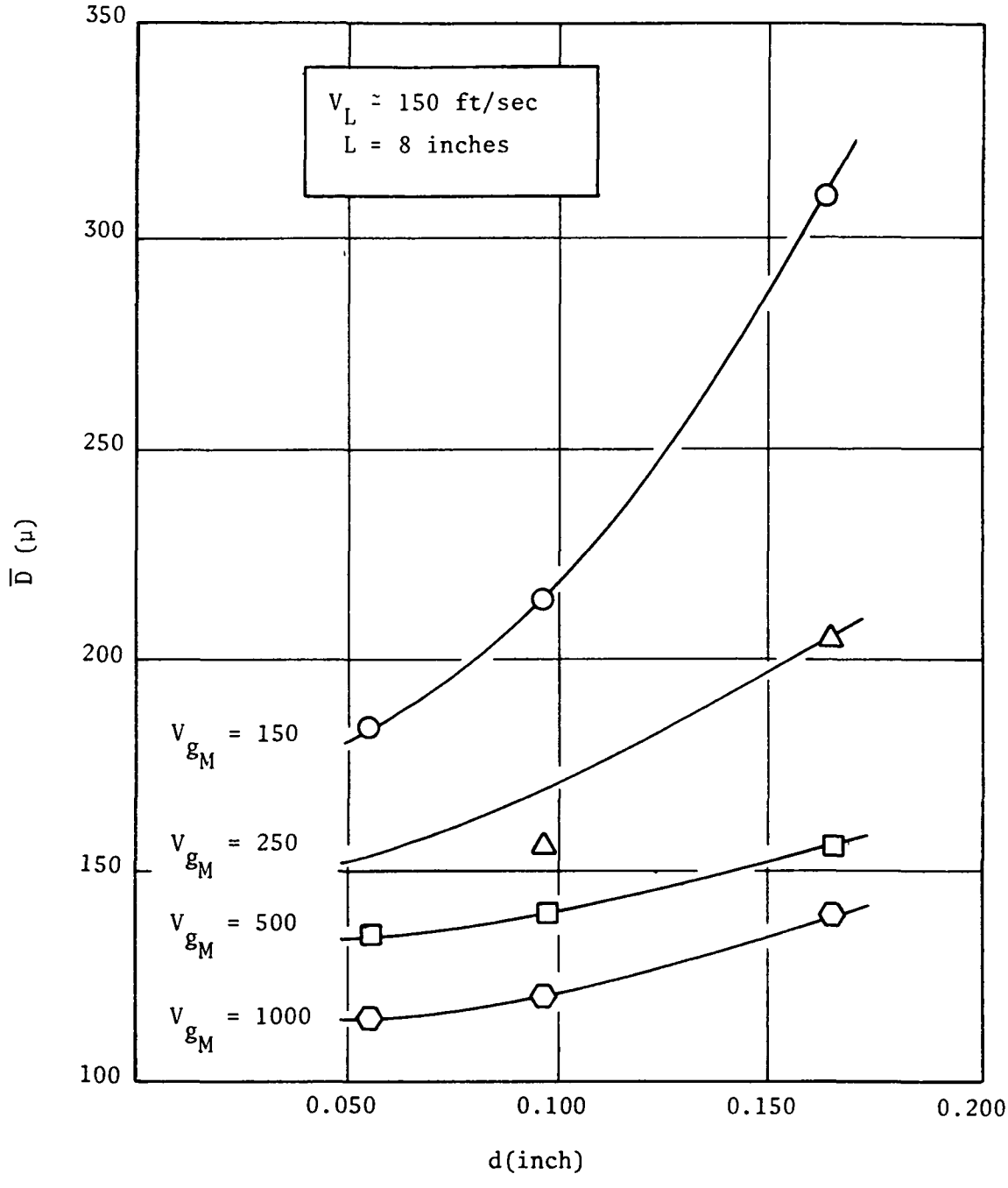

Figure 10. Influence of Injector Orifice Diameter on Mass Median Dropsize Obtained in Accelerating Gas Flowfield

resulting mass median dropsize as the gas velocity is increased. For example, at a gas velocity of 500 ft/sec, a threefold increase in the diameter produces only about a 15 -percent change in the dropsize as compared to a 70-percent increase at a gas velocity of 150 ft/sec.

The influence of the liquid injection velocity is closely tied with the value of gas velocity because of the dropsize dependence on the relative gas-to-liquid velocity difference. However, at values of V_g greater than or equal to the liquid injection velocity, the tendency is for the dropsize to decrease with increasing V_L (with other parameters constant). This is shown in Fig. 11 which presents the data obtained with the 0.055-inch-diameter elements (Fig. 11a) and the 0.094-inch-diameter elements (Fig. 11b) as a function of the injection velocity.

DROPSIZE DISTRIBUTION RESULTS

An examination of the dropsize distributions corresponding to the mass median dropsizes presented above showed that they had essentially the same characteristics as those obtained in the study of the secondary atomization process (Ref. 8). This is to be expected since the mass median dropsizes exhibit trends also similar to those reported in Ref. 8. As was observed in that study, the dropsize distribution tended to become more nearly monodisperse as the mass median dropsize was decreased. This result was found to be essentially independent of the parametric variation that produced the decrease in the mean dropsize.

It was reported in Ref. 8 that no distribution could be found that would fit all of the data over the entire range of droplet sizes. However, a function which does provide a good fit to the data is the Rosin-Rammler distribution function (Ref. 10):

$$\frac{d(\dot{w}/\dot{w}_{TOT})}{d(D/\bar{D})} = \frac{2.46\ (D/\bar{D})^{1.46}}{(1.21)^{2.46}} \exp\left[-\frac{(D/\bar{D})^{2.46}}{1.61}\right] \tag{7}$$

This function was particularly effective in fitting the part of the distribution above $D/\bar{D} = 1$. This is shown in Fig. 12 where two typical distributions are presented. These distributions were produced by the 0.094-inch-diameter element at an injection velocity of 142 ft/sec but at two different gas velocities. The distance from the injector was the same in both cases, i.e., 8 inches.

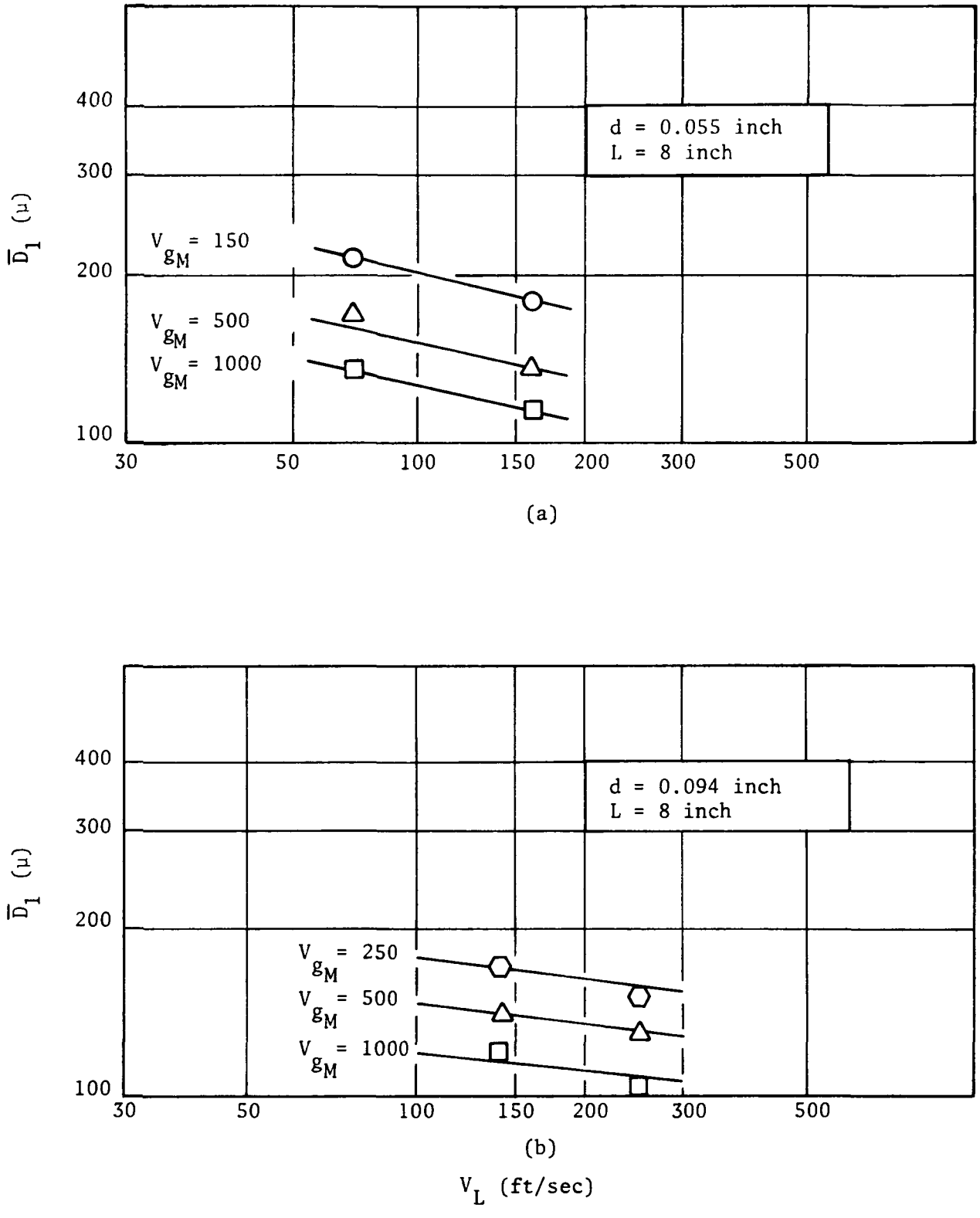

Figure 11. Influence of Liquid Injection Velocity on the Mass Median Dropsize Obtained in Accelerating Gas Flowfield

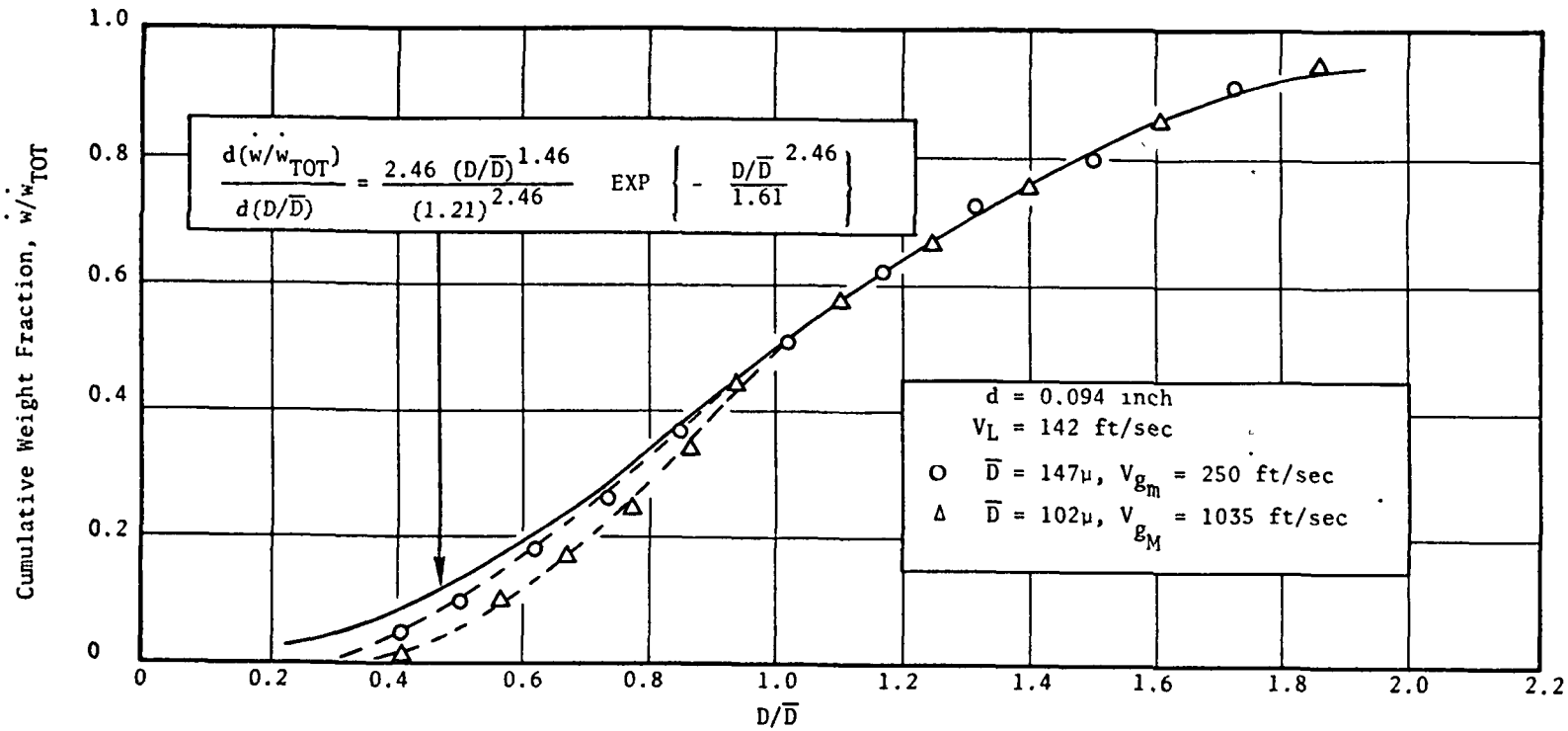

Figure 12. Comparison of Experimental Data to Rosin-Rammler Normalized Distribution Function

Page Intentionally Left Blank

5.0 DISCUSSION

The experimental data presented in the preceding section represent the results of one portion of a two-part study of the effects of an accelerating gas flow on spray atomization.

In both studies, the spray was produced by single-element, like-doublet, impinging stream injectors that are typical, in terms of geometry and liquid velocity, of those used in rocket engines. The gas velocities and distances over which the gas is accelerated are also typical of rates of acceleration of the combustion gases in rocket engine combustion chambers. Thus, the results should be directly applicable to rocket engine performance calculations.

The other part of the study (Ref. 8) dealt with the breakup of droplets by accelerating the gas carrying the spray after the spray had been formed. This process of droplet breakup has been termed secondary atomization. The study described in this report was concerned with the spray dropsize distributions that are produced by accelerating the gas flow during the formation of the spray. This has been termed the primary atomization process since the accelerating gas acts on the liquid jets, sheets, and ligaments and, hence, governs the size of the droplets that are initially formed.

It is possible, conceptually, to differentiate the atomization processes. In reality, however, the primary atomization process will include the effects of droplet breakup, i.e., secondary atomization, since the formation of the droplet spray is not an instantaneous occurrence. That is, for some distance downstream of the injector, both ligaments and drops will exist and droplet breakup will occur simultaneously with droplet formation from ligaments. In fact, the results have shown that at distances sufficiently far from the injector, the median dropsize is governed primarily by droplet breakup and the effects of the gas on the disintegration of sheets and ligaments can be neglected. The evidence supporting this is that, under identical gas and liquid flowrates and velocities, the so-called "primary" dropsize approaches the measured "secondary" dropsize when L is large. Because of this similarity, much of the discussion of the secondary atomization process presented in Ref. 8 is applicable to the results of this study, and the reader is referred to that report for additional aspects of the results.

The principal difference between the dropsizes measured in the two studies was the effect of length on the results. In the Ref. 8 study, it was found that the length of the acceleration zone did not significantly affect the results, indicating that the breakup times are very short compared to the time the droplets spend in the acceleration zone. In this study, however, distance did have an effect. As shown in Fig. 6, for example, the dropsize increased when the exposure length, L, to the accelerating gas velocity was decreased.

Based on the results of Ref. 8, this increase in dropsize cannot be explained in terms of droplet breakup time. Rather, the increase in dropsize must be interpreted as a qualitative measure of the distance required for the droplet

spray to be completely formed. Thus, with short acceleration distances, the gas is acting primarily on the liquid sheet and ligaments and, to a lesser extent, on the droplets formed from the ligaments. In addition, close to the injector face, the liquid is concentrated in the center of the test section and the closely spaced drops and ligaments could be shielding each other to a greater extent than at larger distances.* This would then tend to prevent the droplets that are formed early from undergoing additional atomization.

EMPIRICAL CORRELATION OF THE RESULTS

The empirical correlations that were developed from the data obtained in this study were presented with the experimental results in the preceding section. It was shown there that the primary dropsize can be related to the secondary dropsize through the empirical correlation:

$$\bar{D}_1 = \tau \bar{D}_2 \qquad (6)$$

when $\bar{D}_2$ is given by either Eq. 2 or 3, while the parameter τ (which is ≥ 1) is expressed by Eq. 5. As was shown in Fig. 6 through 9, the empirical correlations provide a good fit to the experimental data. As can be seen from Eq. 2 and 3, the secondary dropsize, $\bar{D}_2$, is a function of two parameters, $\bar{D}_c$ and $\Delta V/V_L$.

If Eq. 1 (i.e., the empirical correlation for the dropsize in a static environment, $\bar{D}_o$) is introduced into the expression for $\bar{D}_c$ (Eq. 4), it is found that:

$$\bar{D}_c = 8\, \bar{D}_o^{0.66}/V_L^{0.09} \qquad (7)$$

Thus, if the small effect of V_L is neglected, the primary dropsize, $\bar{D}_1$, is seen to be a function of the characteristic dropsize of the injector, $\bar{D}_o$, the nondimensional velocity, $\Delta V/V_L$, and the parameter τ.

The secondary dropsize, $\bar{D}_2$, or equivalently, the primary dropsize $\bar{D}_1$ at $L = \infty$, is shown in Fig. 13 as a function of the characteristic dropsize $\bar{D}_o$ for various values of $\Delta V/V_L$. As shown there, the dropsize, $\bar{D}_2$, decreases as the gas velocity is increased with fixed injector parameters, i.e., constant $\bar{D}_o$ and V_L. It also shows that a limiting value of $\bar{D}_2$ is obtained as both $\bar{D}_o$ and $\Delta V/V_L$ are increased. The effect of V_L independent of its contribution to $\bar{D}_o$ and $\Delta V/V_L$ is seen (dashed lines in Fig. 13) to be small for low values of $\Delta V/V_L$, and totally negligible for large values of $\Delta V/V_L$.

*It was noted in Ref. 8 that, if the droplets are spread uniformly through the gas, the mean droplet spacing would be on the order of 6 to 13 droplet diameters. However, close to injector face, the spacing is more on the order of half of this, i.e., 3 to 6 diameters, since the spray is still spreading outward from the impingement point. Thus, at 2 inches from the injector face, the cross section of the spray, assuming a 60-degree fan, is about 2 to 3 in.^{2} (i.e., an order of magnitude less than the cross section available to the gas flow, 20 in.^{2}).

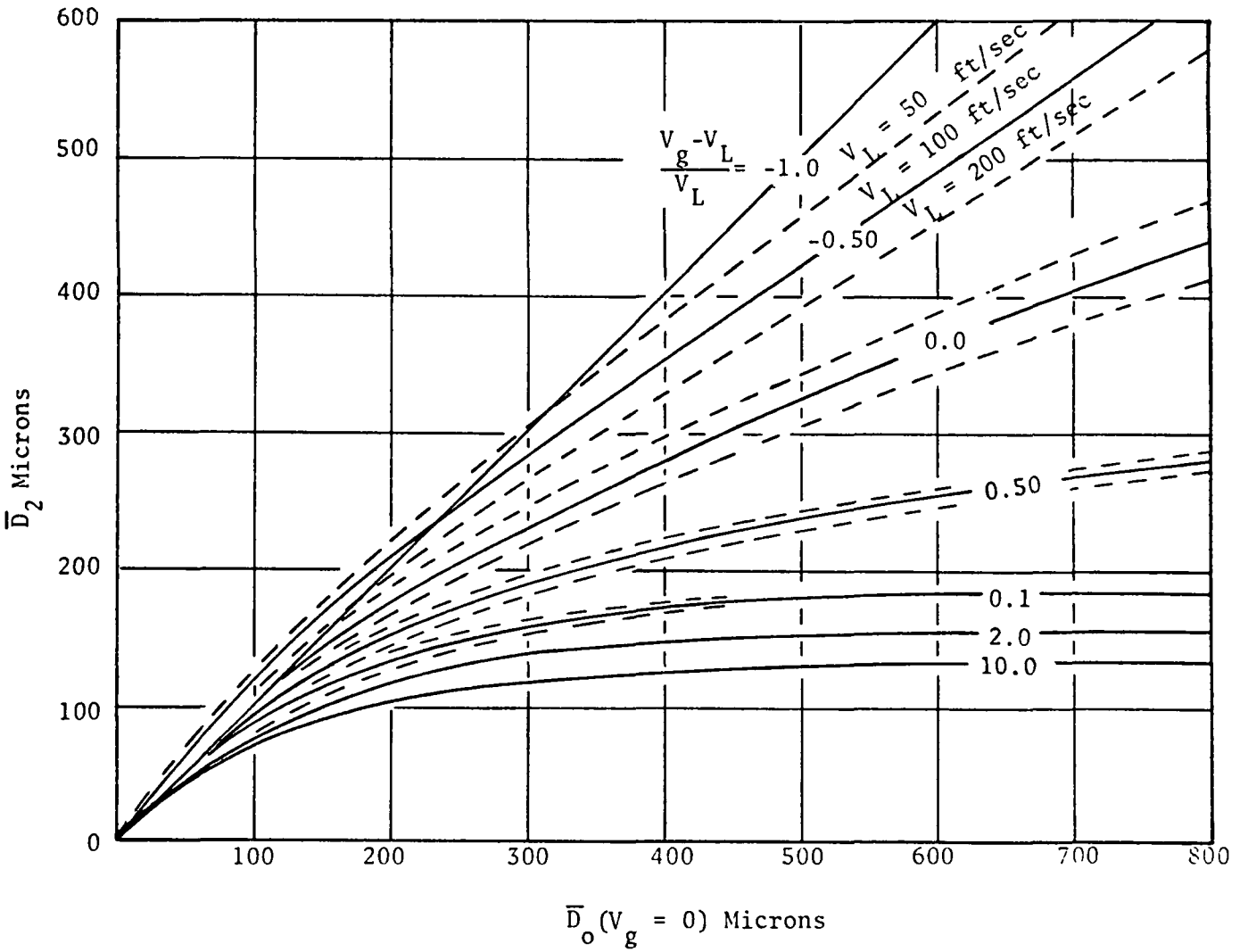

Figure 13. Plot of the Empirical Correlations, L = ∞ (τ = 1)

The effect of length on the parameter τ is illustrated in Fig. 14. For these calculations, an orifice diameter of 0.094 inch and an injection velocity of 100 ft/sec were selected. According to Eq. 1, the characteristic dropsize of the injector at these conditions is 415 microns. Figure 14 shows the result exhibited by the experimental data in that τ, and hence the dropsize $\overline{D}_1$, increase when the maximum gas velocity is attained closer to the injector face (shorter exposure distance). It also shows that, as the gas velocity is increased, the effect of length becomes of lesser importance.

The above correlations, together with the normalized dropsize distribution function expressed by Eq. 7, are sufficient to completely characterize the dropsize distribution for the range of experimental parameters examined. However, the empirical correlations should not be used outside the range in which data were obtained. Specifically, $\overline{D}_o$ should be limited to values of 200 to 600 microns.* In terms of $\overline{D}_c$, which incorporates the range of orifice diameters and injection velocities examined, the limits should be $140 \leq \overline{D}_c \leq 360$ microns. The length, L, should be not less than 2 inches. Fortunately, most rocket engine combustors will have values of these parameters within the prescribed ranges.

APPLICATION OF RESULTS TO COMBUSTION MODELS

In Ref. 8, it is recommended that the simplest approach to incorporating the results of that study to combustion model computer codes would be to simply correct the initial dropsize according to the empirical correlations for $\overline{D}_2$. The results obtained here do not indicate a necessity to change that recommendation. However, to incorporate the effect of chamber length, it is recommended that the correlations presented in this report should be utilized.

*Includes the data obtained in Ref. 8

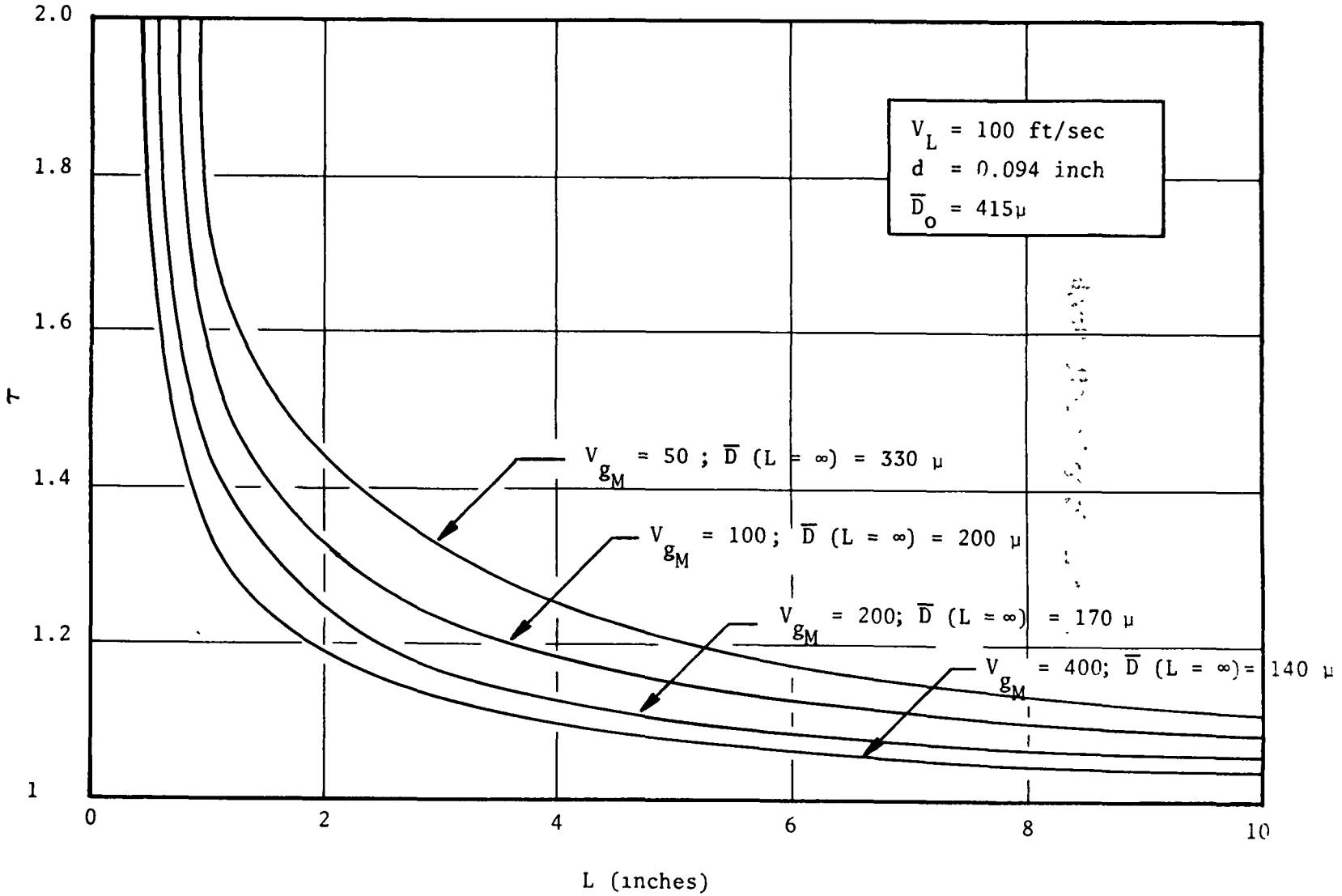

Figure 14. Influence of Length on the Parameter τ

Page Intentionally Left Blank

6.0 CONCLUDING REMARKS AND RECOMMENDATIONS

The objective of this study was to determine quantitatively the influence of an accelerating gas flow on the atomization characteristics of impinging stream injectors and to develop, from the experimental data, droplet breakup criteria that can be readily incorporated into combustion models for the calculation of rocket engine combustion performance. This objective has been achieved.

From the experimental data obtained in this study, it can be concluded that the acceleration of the combustion gas in the early stages of the combustion process will significantly enhance the atomization of liquid propellants. Failure to account for this additional atomization could lead to underprediction of combustion performance.

It is further concluded that the parameters having the greatest effect on the resulting spray median dropsize are the injector parameters of orifice diameter and injection velocity, the maximum gas velocity, and the distance from the injector at which this maximum gas velocity is achieved. In the limit of large distances from the injector, the effect of length can be neglected. In this case, the resulting dropsizes approach those measured in the Ref. 8 study of secondary atomization.

Additional aspects of the effects of an accelerating gas flow on droplet breakup are presented in Ref. 8. Recommendations for future work in this area also are presented in the Ref. 8 report.

Page Intentionally Left Blank

APPENDIX A

REFERENCES

1. Priem, R. J. and M. F. Heidmann, Propellant Vaporization as a Design Criterion for Rocket Engine Combustion Chambers, NASA TR R-67, National Aeronautics and Space Administration, Washington, D.C., 1960.

2. Lambiris, S., L. P. Combs, and R. S. Levine, "Stable Combustion Processes in Liquid Rocket Engines," Combustion and Propulsion, Fifth AGARD Colloquium, High Temperature Phenomena, pp. 569-634, MacMillan, New York, New York, 1963.

3. Dickerson, R. A., K. Tate, and W. Nurick, Correlation of Spray Injector Parameters with Rocket Engine Performance, AFRPL-TR-68-11, Rocketdyne Division, Rockwell International, Canoga Park, Calif., January 1968.

4. Reibling, R. W., R. M. Knight, and C. K. Nagai, Chamber Technology for Space Storable Propellants, Task II, Interim Report, Vol. 2, R-6028-2, Rocketdyne Division, Rockwell International, Canoga Park, California, October 1965.

5. Falk, A. Y., S. D. Clapp, and C. K. Nagai, Space Storable Propellant Performance Study, NASA CR-72487, Rocketdyne Division, Rockwell International, Canoga Park, California, November 1968.

6. Nurick, W. H. and R. M. McHale, Noncircular Orifice Holes and Advanced Fabrication Techniques for Liquid Rocket Injectors, Phase I, NASA CR-108570, Rocketdyne Division, Rockwell International, Canoga Park, California, November 1970.

7. Arbit, H. A., S. D. Clapp, and C. K. Nagai, Lithium-Fluorine-Hydrogen Propellant Investigation, NASA CR-72695, Rocketdyne Division, Rockwell International, Canoga Park, California, May 1970.

8. Zajac, L. J., Droplet Breakup in Accelerating Gas Flows, Part II: Secondary Atomization, NASA-CR-134479, Rocketdyne Division, Rockwell International, Canoga Park, California, R-9337-2, October 1973.

9. Zajac, L. J., Correlation of Spray Dropsize Distribution and Injector Variables, R-8455, Rocketdyne Division, Rockwell International, Canoga Park, California, February 1971.

10. Rosin, P. and E. Z. Rammler, Ver. Duet. Ing., 71, 1, 1927, J. Inst. Fuel, 1, 29, 1933.

Page Intentionally Left Blank

APPENDIX B

DISTRIBUTION LIST (CONTRACT NAS3-14371)

	Copies
National Aeronautics and Space Administration Lewis Research Center 21000 Brookpark Road Cleveland, Ohio 44135	1
Attn: Dr. R. J. Priem MS 500-209	2
N. T. Musial MS 500-311	1
Library MS 60-3	1
Report Control Office MS 5-5	1
L. Gordon, MS 500-209	1
E. O. Bourke MS 500-209	1
Rockets and Spacecraft Procurement Section MS 500-313	1
E. W. Conrad MS 500-204	1
Brooklyn Polytechnic Institute Attn: V. D. Agosta Long Island Graduate Center Route 110 Farmingdale, New York 11735	1
Chemical Propulsion Information Agency Johns Hopkins University/APL Attn: T. W. Christian 8621 Georgia Avenue Silver Spring, Maryland 20910	1
NASA Scientific and Technical Information Facility Attention: Acquisitions Branch P.O. Box 33 College Park, Md. 20740	10
Aerospace Corporation Attn: O. W. Dykema P.O. Box 95085 Los Angeles, California 90045	1
Ohio State University Department of Aeronautical and Astronautical Engineering Attn: R. Edse Columbus, Ohio 43210	1

	Copies
TRW Systems Attn: G. W. Elverum One Space Park Redondo Beach, California 90278	1
Bell Aerospace Company Attn: T. F. Ferger P.O. Box 1 Mail Zone J-81 Buffalo, New York 14205	1
Pratt & Whitney Aircraft Florida Research & Development Center Attn: G. D. Garrison P.O. Box 710 West Palm Beach, Florida 33402	1
Purdue University School of Mechanical Engineering Attn: R. Goulard Lafayette, Indiana 47907	1
Air Force Office of Scientific Research Chief Propulsion Division Attn: Capt. L. R. Lawrence, Jr. (NAE) 1400 Wilson Blvd. Arlington, Virginia 22209	1
Pennsylvania State University Mechanical Engineering Department Attn: G. M. Faeth 207 Mechanical Engineering Bldg. University Park, Pennsylvania 16802	1
University of Illinois Aeronautics/Astronautics Engineering Department Attn: R. A. Strehlow Transportation Bldg., Room 101 Urbana, Illinois 61801	1
NASA Lyndon B. Johnson Space Center Attn: J. G. Thibadaux Houston, Texas 77058	1
Massachusetts Institute of Technology Department of Mechanical Engineering Attn: T. Y. Toong 77 Massachusetts Avenue Cambridge, Massachusetts 02139	1

	Copies
Illinois Institute of Technology Attn: T. P. Torda Room 200 M. H. 3300 S. Federal Street Chicago, Illinois 60616	1
AFRPL Attn: R. R. Weiss Edwards, California 93523	1
U.S. Army Missile Command AMSMI-RKL, Attn: W. W. Wharton Redstone Arsenal, Alabama 35808	1
University of California Aerospace Engineering Department Attn: F. A. Williams P. O. Box 109 LaJolla, California 92037	1
Georgia Institute of Technology Aerospace School Attn: B. T. Zinn Atlanta, Georgia 30332	1
Ultrasystems Attn: T. J. Tyson 2400 Michelson Drive Irvine, California 92664	1
Mr. Donald H. Dahlene U.S. Army Missile Command Research, Development, Engineering and Missile Systems Laboratory Attn: AMSMI-RK Redstone Arsenal, Calabama 35809	1
TISIA Defense Documentation Center Cameron Station Building 5 5010 Duke Street Alexandria, Virginia 22314	1
Office of Assistant Director (Chemical Technology) Office of the Director of Defense Research and Engineering Washington, D.C. 20301	1
D. E. Mock Advanced Research Projects Agency Washington, D.C. 20525	1

	Copies
Dr. H. K. Doetsch Arnold Engineering Development Center Air Force Systems Command Tullahoma, Tennessee 37389	1
Library Air Force Rocket Propulsion Laboratory (RPR) Edwards, California 93523	1
Library Bureau of Naval Weapons Department of the Navy Washington, D.C.	1
Library Director (Code 6180) U.S. Naval Research Laboratory Washington, D.C. 20390	1
APRP (Library) Air Force Aero Propulsion Laboratory Research and Technology Division Air Force Systems Command United States Air Force Wright-Patterson AFB, Ohio 45423	1
Rockwell International Rocketdyne Division Attn: L. P. Combs, D/578 MS BA 17 6633 Canoga Ave. Canoga Park, California 91304	1
Technical Information Department Aeronutronic Division of Philco Ford Corporation Ford Road Newport Beach, California 92663	1
Library-Documents Aerospace Corporation 2400 E. El Segundo Blvd. Los Angeles, California 90045	1
Princeton University James Forrestal Campus Library Attn: D. Harrje Post Office Box 710 Princeton, New Jersey 08540	1
U.S. Naval Weapons Center Attn: T. Inouye, Code 4581 China Lake, California 93555	1

	Copies
Office of Naval Research Navy Department Attn: R. D. Jackel, 473 Washington, D.C. 20360	1
Air Force Aero Propulsion Laboratory Attn: APTC Lt. M. Johnson Wright Patterson AFB, Ohio 45433	1
Naval Underwater Systems Center Energy Conversion Department Attn: Dr. R. S. Lazar, Code TB 131 Newport, Rhode Island 02840	1
NASA Langley Research Center Attn: R. S. Levine, MS 213 Hampton, Virginia 23365	1
Aerojet General Corporation Attn: David A. Fairchild, Mech. Design Post Office Box 15847 (Sect. 9732) Sacramento, California 95809	1
Colorado State University Mechanical Engineering Department Attn: C. E. Mitchell Fort Collins, Colorado 80521	1
University of Wisconsin Mechanical Engineering Department Attn: P. S. Myers 1513 University Avenue Madison, Wisconsin 53706	1
Rockwell International Rocketdyne Division Attn: J. A. Nestlerode, AC46, D/596-121 6633 Canoga Avenue Canoga Park, California 91304	1
University of Michigan Aerospace Engineering Attn: J. A. Nicholls Ann Arbor, Michigan 48104	1
Tulane University Attn: J. C. O'Hara 6823 St. Charles Ave. New Orleans, Louisiana 70118	1

	Copies
University of California Department of Chemical Engineering Attn: A. K. Oppenheim 6161 Etcheverry Hall Berkeley, California 94720	1
Sacramento State College School of Engineering Attn: F. H. Reardon 6000 J. Street Sacramento, California 95819	1
Purdue University School of Mechanical Engineering Attn: B. A. Reese Lafayette, Indiana 47907	1
NASA George C. Marshall Space Flight Center Attn: R. J. Richmond, SNE-ASTN-PP Huntsville, Alabama 35812	1
Jet Propulsion Laboratory California Institute of Technology Attn: J. H. Rupe 4800 Oak Grove Drive Pasadena, California 91103	1
University of California Mechanical Engineering Thermal Systems Attn: Prof. R. Sawyer Berkeley, California 94720	1
ARL (ARC) Attn: K. Scheller Wright Patterson AFB, Ohio 45433	1
Library Bell Aerosystems, Inc. Box 1 Buffalo, New York 14205	1
Report Library, Room 6A Battelle Memorial Institute 505 King Avenue Columbus, Ohio 43201	1
D. Suichu General Electric Company Flight Propulsion Laboratory Dept. Cincinnati, Ohio 45215	1

	Copies
Library Ling-Temco-Vought Corp. P.O. Box 5907 Dallas, Texas 75222	1
Marquardt Corp. 16555 Saticoy Street Box 2013--South Annex Van Nuys, Calif. 91409	1
P. F. Winternitz New York University University Heights New York, N. Y.	1
R. Stiff Propulsion Division Aerojet-General Corp. P.O. Box 15847 Sacramento, California 95803	1
Library, Dept. 596-306 Rockwell International Rocketdyne Division 6633 Canoga Ave. Canoga Park, California 91304	1
Library Stanford Research Institute 333 Ravenswood Ave. Menlo Park, California 94025	1
Library Susquehanna Corp. Atlantic Research Division Shirley Highway and Edsall Rd. Alexandria, Va. 22314	1
STL Techn. Lib. Doc. Acquisitions TRW System Group 1 Space Park Redondo Beach, California 90278	1
Dr. David Altman United Aircraft Corp. United Technology Center P.O. Box 358 Sunnyvale, California 94088	1

	Copies
Library United Aircraft Corp. Pratt & Whitney Division Florida Research and Development Center P.O. Box 2691 W. Palm Beach, Fla. 33402	1
Library Air Force Rocket Propulsion Laboratory (RPM) Edwards, California 93523	1
Kenneth R. Purdy, Professor P.O. Box 5014 Tennessee Technological University Cookeville, Tennessee 38501	1